Smart Structures and Systems, *Vol. 20, No. 5 (2017) 539-548*
DOI: https://doi.org/10.12989/sss.2017.20.5.539

Causes of uncertainty in thermoelasticity measurements of structural elements

Roberto Marsili[a], Gianluca Rossi[b] and Emanuela Speranzini[*]

Department of Engineering, via G. Duranti, 93 – 06125 Perugia, Italy

(Received June 18, 2017, Revised August 12, 2017, Accepted September 3, 2017)

Abstract. Thermoelasticity is a contactless technique for measuring stress distributions in structural elements stressed by dynamic loads. This work describes the characteristics, analyzes the main causes of uncertainty and illustrates a series of operative methods for reducing its effects. More specifically, the effects of the angle of view between the thermographic camera and the surface of the object are studied, along with those due to the heat transmission by conduction between the various parts of the thing being measured as a function of the stress frequencies. The analyses, both theoretical and experimental, are aimed at defining the operational limits and optimal measurement and test conditions in relation to the measurement uncertainty that is considered tolerable in the specific application.

Keywords: thermoelasticity; monitoring; uncertainty analysis; stress distribution measurement; thermography

1. Introduction

Thermoelasticity is a technique used to measure the state of stress that is not destructive and is based on the capturing of infrared images. Infrared radiation (IR) is in fact that which is of interest in the study of thermoelasticity, since the radiation emitted by bodies at room temperature falls precisely within the range of the spectrum from 0.76 to 1000 µm; only at temperatures above 800 kelvin do objects begin to emit radiation in the visible range in appreciable amounts (Barone and Patterson 1998). Depending on the degree of molecular agitation, the IR spectrum can be divided into three main regions: near IR (wavelengths from 0.78 to 1.5 µm), mid IR (1.5 to 20 µm) and far IR (20 to 1000 µm). The most interesting range for nondestructive thermographic tests is the near and mid IR, in the infrared radiation band with wavelengths between 0.75 and 14 microns. The measurement of this radiation allows one to obtain the surface temperature of the bodies, and therefore by using a thermal camera it is possible to trace the thermal map of the "scene" framed through the interpretation of the radiation perceived by the detector, which is the sensitive element (D'Emilia *et al*. 2011, 2013, Rossi *et al.* 2009, Zanetti *et al*. 2010, Logozzo *et al.* 2014).

Thermoelastic infrared analysis can be applied to the study of materials and structures mainly in two ways: thermoelastic stress analysis, to visualize and measure stresses in structural elements under stress (Harwood and Cummings 1991), and in nondestructive tests to obtain information and images regarding defects (the defect generates an alteration of the thermal field) such as thermal irregularities caused by cracks (Speranzini and Agnetti 2014, 2013), bonding, gaps, material discontinuities, porosity, and delamination (Speranzini and Agnetti 2012, 2016) as in the case of composite materials (Speranzini and Tralascia 2010), which may compromise the mechanical strength of a structure (Wong *et al*. 1988, Arefi and Zenkour 2017).

One of the main advantages of this technique is that it makes it possible to analyze the temperature of any body without coming into contact with it, i.e., in a noninvasive manner, allowing the measurements to be repeated over time. Moreover, it requires no surface preparation (except in the case of shiny metal surfaces), it allows the inspection of large surfaces in a short time, it does not use harmful radiation and, in contrast to X-rays, as it can work by reflection, it does not require the body to be accessible from both surfaces. The technique is applicable in a wide variety of fields and situations: in the mechanical industry (Cardelli *et al*. 2015, Garinei and Marsili 2014b, Brouckaert *et al*. 2012), aeronautics (Garinei and Marsili 2012, 2013), automotive (Grigg *et al*. 2000), components and structures can be analyzed both in production and in use; in civil buildings it is highly valued because it is a contactless, noninvasive, is easy-to-use investigative technique for the historical and artistic heritage as an alternative to other methods (Speranzini *et al*. 2017, Garinei and Marsili 2014a, Kim *et al*. 2017, Ezzat, *et al*. 2016, Zhou *et al*. 2016, Garg *et al*. 2016).

In thermoelastic analysis, once the surface temperature of the loaded structural element has been measured, it is possible to directly determine the state of stress through the stress invariant, which is the sum of the main stress

*Corresponding author, Professor
E-mail: emanuela.speranzini@unipg.it
[a] Professor
E-mail: roberto.marsili@unipg.it
[b] Professor
E-mail: gianluca.rossi@unipg.it

http://www.techno-press.com/journals/sss&subpage=7 ISSN: 1738-1584 (Print), 1738-1991 (Online)

components. It has been shown that it can provide quantitative results in accordance with the values provided by strain gauges (D'Emilia *et al.* 2015), compared to which this system has the advantages of being able to inspect the entire visible surface of a structural element, of having greater spatial resolution in reading the stress concentration peaks, and of not having complex shape problems that could prevent the attaching of the instruments. However, in a thermoelastic system, there may be several causes of measurement uncertainty, above all the many interference inputs unrelated to the thermoelastic effect, which vary the surface temperature of the stressed structural elements.

In this work the main causes of uncertainty (D'Aponte *et al*. 2015) are analyzed and a series of operative methods for reducing its effects are illustrated in accordance with standard normative (Lesniak 1993, UNI CEI ENV 13005 (2000)). More specifically, the effects of the angle of view between the thermal camera and the surface of the object are studied, along with those due to the heat transmission by conduction between the various parts of the object being measured according to the stress frequencies. The theoretical and experimental analyses performed made it possible to define quantitatively the operational limits and optimal conditions for measurements and tests for the most common usage situations, in relation to the measurement uncertainty that is considered tolerable in the specific application.

2. The principle of thermoelastic measurement

The thermoelastic effect is the variation in temperature generated on the material of a structural element when it is stressed by dynamic loads (Rocca and Bever 1950, Sakagami *et al.* 1995, Szolwinski *et al*. 1999). This physical phenomenon is well-known for gases, which vary in temperature if subjected to a change in pressure. The thermoelastic effect is generated in solids by the first invariant of the stress σ, which on the surface of an object can be calculated as the sum of two stresses that are in orthogonal directions from each other. A variation in the time $\Delta\sigma$ of the first invariant generates a variation in the time of the temperature ΔT which can be obtained, through a series of hypotheses (material is homogeneous, linear, isotropic, etc.), from the classic equation in Barone and Patterson (1998) and Offerman *et al.* (1997)

$$\Delta\sigma = -\frac{\rho C_p}{\alpha}\frac{\Delta T}{T} \tag{1}$$

where ρ is the density of the material, C_p is its specific heat, and α is its thermal conductivity. Thus it is possible to determine the stress condition of a solid body based on the detection of this temperature variation. It can be calculated from Eq. (1) that, for common steel, a stress variation of 1 MPa corresponds to a temperature variation of about 1 mK, and a stress variation up to its yielding point corresponds to a temperature variation of about 0.2 K (Harish *et al.* (2000), Ju *et al.* (1997). Therefore the temperature variations produced by the thermoelastic effect must be measured within a small range with a very high resolution. To achieve this, low-noise thermal sensors are used along with the lock-in technique in processing the output signal from the temperature-sensitive elements, as is better explained in following. In order to obtain a contactless measurement technique for stress maps, a thermal camera may be used for the detecting of temperature variations.

Thermal cameras are known, however, to be sensitive to thermal radiation, which in turn is related to temperature by the laws on radiation, by emissivity, by the surface characteristics in general, and by the angle from which it is observed. For example, a gray body with absolute T temperature generates an irradiance J, given by the well-known equation

$$J = \alpha\sigma_0 T^4 \tag{2}$$

where α is the emissivity of the body, supposedly grey, T is its absolute temperature and σ_o is the Stefan-Boltzmann constant. If T varies in time by ΔT from the previous equation, a corresponding variation in the thermal output emitted ΔJ can be determined. In a thermal camera, this variation in thermal radiation is collected by an infrared optical system characterized by an aperture with diameter D and a focal length f. If the measurement surface that emits the thermal power is at an infinite distance from the optical system, and the infrared sensor, upon which the radiated energy converges, has a diameter of d', then the radiant thermal power $\Delta J_{DETECTOR}$ arriving at the sensor is (from Rossi *et al.* 2009)

$$\Delta J_{DETECTOR} = \frac{D^2 d'^2}{4f^2}\Delta J \tag{3}$$

One great advantage to using a thermal camera is the absence of perturbations in the temperature range, and thus in the stresses to be measured. Another strong point for a thermal camera is the high response speed to dynamic inputs. The resolution that can be obtained, however, is limited by the noise level of the best infrared (IR) sensors available, which in the best conditions is rarely less than the thermal equivalent of 10 mK. However, in the development of the thermoelastic measurement technique, it was possible to solve this problem by adopting special methods for processing the signal of the IR sensors, correlating their output with the load signal, making use of the well-known lock-in amplifiers technique. This has made it possible to reduce the effects of noise and to achieve a high thermal resolution – obviously only for the measurement of average values of thermal fluctuation amplitudes. To complete the picture of the main relationships of a thermoelastic measurement chain, the typical expression of the signal-to-noise ratio of the IR sensors is given, based on the parameter D^*, commonly defined as the signal-to-noise ratio when the sensor is affected by 1 W of power, it has a sensitive area of 1 cm^2, and the noise is measured with a bandwidth Δf of 1 Hz. The noise level in equivalent thermal power NEP can thus be expressed as

$$NEP = \frac{d' \Delta f^{\frac{1}{2}}}{D^*} \tag{4}$$

For an evaluation of the main components of the signal-to-noise ratio *S / N* of a thermoelastic system, the following expression can be written, which shows how the main parameters affect the infrared optical system, the object being measured and the measurement system

$$S / N = \Delta J_{DETECTOR} / NEP = \frac{D^2 d' D^*}{4 f^2 \Delta f^{\frac{1}{2}}} \Delta J \tag{5}$$

A classic thermographic system suitable for measuring the temperature distribution over the surface of an object generally does not allow a measurement of its oscillation amplitude with the degree of resolution normally required to apply the thermoelastic principle. Thus it was necessary to develop special thermographic instruments. Specific hardware and software is used that allow a thermal camera to capture and process successive thermal images repeatedly and synchronously, and to store only one that represents the average amplitude of variation over time of the temperature on the points of the surface of the object framed. This type of system is called a differential thermographic camera. Due to the difficulty of knowing all the parameters of the previous expressions, and especially the emissivity of the object's surface, its dependence on the wavelength of the thermal radiation emitted, its dependence on the angle of view, and how thermal exchanges have an effect, in practice the system is calibrated for a direct comparison with the stresses measured in one point of the mechanical component. The strain gauge technique can be used to determine the linear deformations ε_x and ε_y in two perpendicular directions x and y in a small area of uniform stress. The calibration factor *k* can thus be defined as follows

$$\mathrm{k} = \frac{\sigma_x + \sigma_y}{S_{avg}} \tag{6}$$

where S_{avg} is the average spatial output of the grey level of the differential thermographic camera pixels that measure the temperature fluctuation amplitude (or rather, the irradiation ΔJ) in the area of application of the strain gauges. From the known constitutive laws we get the following expression for *k*

$$\mathrm{k} = \frac{E(\varepsilon_X + \varepsilon_Y)}{S_{avg}(1-\nu)} \tag{7}$$

being *E* the modulus of elasticity and ν the Poisson coefficient of the material of the stressed object.

Once factor *k* is determined, it will be possible for that material and for the differential thermographic camera used to go from the output grey level of each pixel to a value of the first stress invariant expressed in MPa.

3. Causes of uncertainty in thermoelasticity

The main causes of uncertainty in a thermoelastic system are first of all the many interference inputs that are unrelated to the thermoelastic effect, which vary the surface temperature of the stressed structural element. However, by using the lock-in technique during processing, only those temperature variations that occur with the frequency of the load applied are significantly influential. The effect of thermal reflections on the surface of the object being tested, connected with the movement of the object which is obviously at the same frequency as the load, the uneven distribution of the emissivity on the surface and its sometimes too low value can all be considerably reduced by painting the surface of the test object. The paint layer increases the signal-to-noise ratio because it increases the emissivity and, if opaque to infrared, it dramatically reduces thermal reflections but unfortunately introduces a "load effect" in an intrinsically nonintrusive technique. We consider as modifier inputs all those that can vary the calibration factor k, defined by Eq. (7). The conversion of $\Delta\sigma$ into the output signal of the thermal camera's pixel is carried out by the thermoelastic effect on the object under examination (including the painting), by the means through which the electromagnetic radiation is propagated, and by the thermal camera. The input signal $\Delta\sigma$ undergoes a series of variable conversions that can be outlined as follows:

$$\Delta\sigma \rightarrow \Delta T_{SUP} \rightarrow \Delta T_{PAINT} \rightarrow \Delta J_{PAINT} \rightarrow \Delta J_{DETECTOR} \rightarrow \mathrm{S}$$

where ΔT_{SUP} is the temperature variation on the surface of the specimen underneath the paint during a stress cycle that can be determined with (1); ΔT_{PAINT} is the corresponding temperature variation that occurs during a stress cycle on the surface of the paint "seen" by the camera; ΔT_{PAINT} is the variation in the intensity of the thermal radiation emitted by the paint that can be evaluated with Eq. (2); $\Delta J_{DETECTOR}$ is the variation in the intensity of the thermal radiation that arrives at the IR sensor; and *S* is the grey level representing the output of the IR sensor.

Let us consider the conversion $\Delta\sigma \rightarrow \Delta T_{SUP} \rightarrow \Delta T_{PAINT}$. The object being tested is usually stressed periodically at a certain load frequency. In the compression phase, warmer areas of the paint and of the surrounding environment will be created, and, in the presence of a stress gradient, areas even warmer than other areas of the neighboring body will also be created. This inevitably causes heat exchanges. The loading phase is followed by the unloading phase, which brings about the inversion of the thermal flows. These heat exchanges depend on many parameters, including the gradient of stress and thus of temperature, time, the thermal conductivity of the object being tested, its thermal capacity, the thermal capacity of the paint layer, and the coefficient of thermal exchange between object and environment. An analysis of these phenomena can be found in (Garinei and Marsili 2014a), where a data processing method for reducing its effects is also proposed.

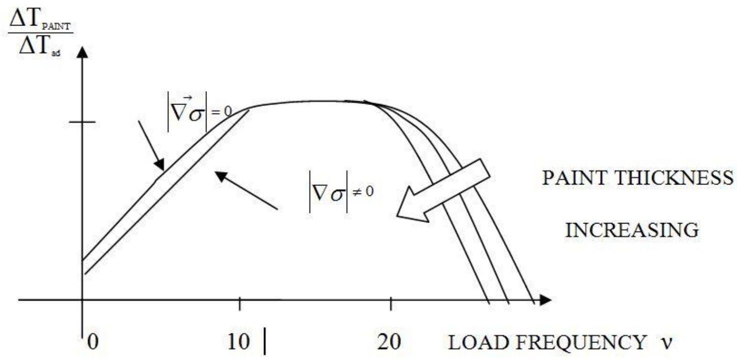

Fig. 1 Qualitative example of the theoretic effects of different disturbance inputs

The heat exchanges' dependence on time allows the load frequency to intervene significantly. As the load frequency increases, the heat has less and less time to propagate. The variation in the paint thickness also changes the thermal exchanges described above, as it determines the thermal capacity. The effect of the load frequency and of paint thickness on heat exchanges lies in the fact that for equal $\Delta\sigma$, we have different values of ΔT_{SUP} *and* ΔT_{PAINT}. Therefore the relationship $\Delta\sigma \rightarrow \Delta T_{SUP} \rightarrow \Delta T_{PAINT}$ will be changed, and participating in the determination of the calibration factor k, it determines its variation. In 1987, McKelvie (Barone and Patterson 1998) developed a relation to determine the attenuation of the temperature produced by thermoelastic effect in the particular case of an infinite plate lying between – l and l above its mean plane, producing even, spatially uniform heat on that mean plane having a sinusoidal time trend. The heat exchange between the stressed object and the paint can be modeled by neglecting the heat lost to the environment, as the latter is several orders of magnitude smaller than that transferred through the paint. If the conductivity of the stressed object is low, the heat that reaches the paint comes from the area of the object immediately underneath it, whose temperature variation undergoes a strong attenuation. As $\Delta T^*_{SUP} > \Delta T^*_{PAINT}$, the signal ΔT^*_{PAINT} will also be attenuated by the heat exchanges. Increasing the thickness of the paint will obviously increase its heat capacity, and therefore the heat exchanged will increase. The decrease in ΔT^*_{PAINT} with the increase in the load frequency is due to the fact that the heat transferred to the paint is reduced, with the stress the specimen is subjected to being the same. Based on these analyses it has been estimated that in steel the signal attenuation due to heat exchanges with the paint usually affects frequencies higher than about 10 Hz, while the attenuation caused by the heat transferred to the outside occurs at frequencies below 10 Hz. This is because the heat transfer by conduction between the stressed object and the paint is much more intense than that by convection between the paint and the environment, and thus it can also take place at high frequencies. This means that while heat is being transferred to the outside, the paint is fully conducting it. When instead the frequency rises and the impedance of the paint starts to have an effect, the heat exchanges between the object and the environment have ceased. Due to the presence of a stress gradient, the transmission of heat within the stressed object is the biggest problem, since it causes an uneven variation in the temperature variation on the surface of the object. In fact there is no generalized decrease in temperature variation with respect to the value in adiabatic conditions, which could be taken into account by determining, for example, the factor k at the same load frequency; rather, there is a decrease in the areas of maximum stress, and an increase in the areas where there is a local minimum of stress. This brings about a spatial variability of the factor k and the danger of underestimating the stress peaks on the object. Also falling within this sphere is the modifier effect of the load frequency, which – as it is able to limit the transmission of heat – has the power of increasing the uniformity of k on the surface of the object.

If we call ΔT_{ac} the variation of temperature that we would have in adiabatic conditions, i.e., due to solely to the thermoelastic effect, the previous analysis allows us to hypothesize a qualitative trend of the curve ΔT / ΔT_{ad} on a generic point of the object, even in the presence of a gradient $\vec{\nabla}\sigma$ as illustrated qualitatively in Fig. 1.

Thus we have a load frequency range (shown in Fig. 1, for example, between 10 and 20 Hz) in which the test and the measurement using the thermoelastic technique can be performed without significant underestimation of the stress levels if the calibration constant k is determined in this frequency range. Then there are two possible areas of underestimation, one at low and the other at high frequencies. In the latter area, the underestimation effect can still be eliminated by doing the calibration at the same test frequency, but this is not possible at low frequencies, because the overall and uniform reduction across the entire surface of the temperature fluctuation is combined also with the further uneven reduction due to the heat transmission between different points of the stressed object due to the gradients of tension and thus of temperature.

4. Designing and construction of the test bench

The theoretical analysis described above, which is based

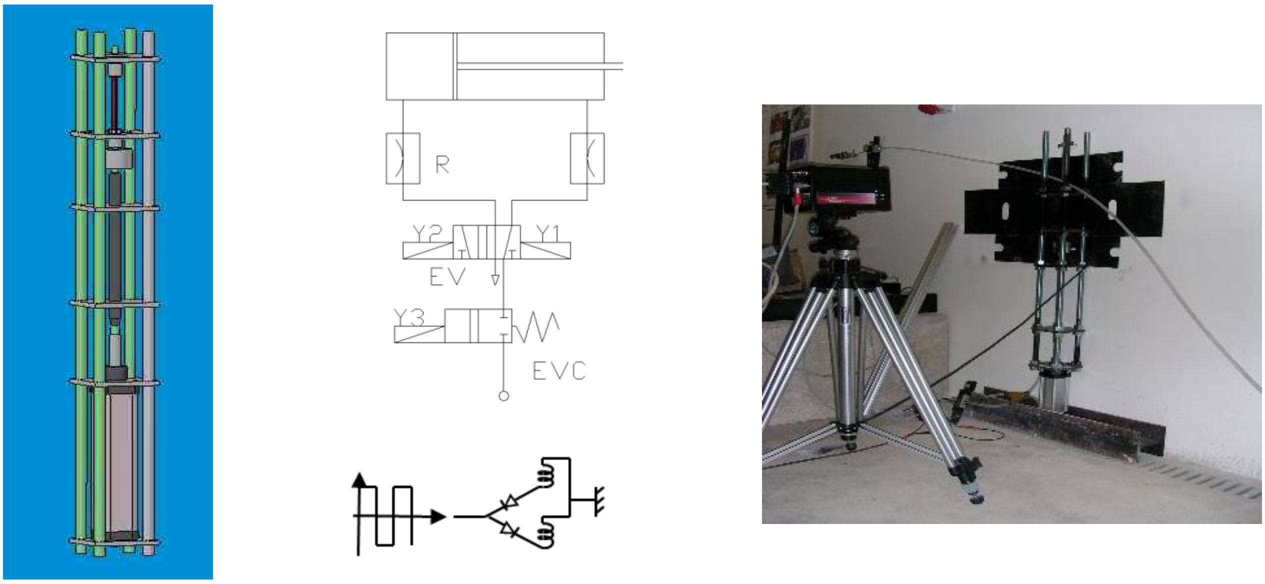

(a) CAD model (b) Pneumatic and electric control circuit (c) Photo of the system built

Fig. 2 The design of the test bench

also on the collection of a series of results available in the bibliography, provides a fairly comprehensive picture for understanding many of the effects of interfering and modifying inputs in a thermoelastic measurement chain. A quantitative evaluation, however, requires knowledge of parameters difficult to determine in practice, such as the thickness of the paint layer and the angular dependence of the emissivity.

For this reason, a specific experimental analysis was conducted in order to have a more reliable evaluation of the performance of the measurement technique in the most typical usage conditions, i.e., using the paints normally applied and the most common materials for the mechanical parts.

The tests planned were aimed at deepening the knowledge on the modifier effect due to the angle of view, its dependence on the type of paint, and the modifier effect due to the loading frequency in the cases where there is uniform stress in the stressed object or there is a stress gradient. Thus the inputs to be varied in the tests are the intensity and frequency of the stress and the angle of rotation of the specimen with respect to the optical axis of the camera. A test bench was thus designed and built that could exert a dynamic axial load on the specimen, in traction and compression, adjustable in both intensity and frequency, and such as to allow the rotation of the specimen during the test. In designing the test bench it was necessary to define the material and the geometry of the specimen, as well as the type and level of stress to be applied. It was intended to be used with a specimen perforated in the center to cause a stress gradient well-known in the literature. The applied load was measured by a transducer with a full scale of 1000 N and a maximum uncertainty of 0.01%, connected with the specimen in series. The maximum load frequency required was limited to 20 Hz, as the phenomena of greatest interest for study take place at low frequencies. The overall CAD 3D model of the test bench designed is shown in Fig. 2. For the actuator, it was decided to use a pneumatic cylinder and to create a specific circuit along with its related power supply and control system. The test bench was then equipped with special grips to allow the rotation of the specimen.

5. Tests performed and discussion

All tests were done using the Delta Therm 1550 differential thermographic camera by Stress Photonics Inc., which has an FPA with 320x256 elements sensitive in the 3-5μm range, made from InSb, capable of capturing up to 1000 thermographic images per second.

5.1 Tests for the analysis of the effects of the angle of view

The purpose of these first tests was to determine how the differential thermographic camera output signal varies with the varying of the angle of view and of the type of paint used. A flat steel specimen was used that was axially loaded in compression and traction. Two series of tests were carried out. In the first series, a parallelepiped-shaped specimen with dimensions of 100 x 10 x 1.2 mm was used, painted with a paint acrylic that we call Type A. The stress cycle is between –200 and +200 N, with a frequency of 10 Hz.

In the second set of tests, the specimen and the stress cycle remain unchanged, and the paint is type B. Measurements were made on each specimen by rotating it from zero to seventy degrees in 5-degree steps. Each measurement was repeated three times. The mean spatial value SAVG of the differential camera output was determined in the central area of thespecimen. The results obtained for paint type A are shown in Fig. 3. For paint type B, the results obtained are shown in Fig. 4.

It is clear that also in the case of the painted surface, the specific angular emissivity is affected by anisotropy. This phenomenon is even more apparent from the following sequenceof images (Fig. 5), in which one notes the gradual attenuation of the measurement systemoutput level with the varying of the angle of view (the color of the central area tends to go from yellow to orange, showing a reduction in the measured output level).

Another interesting phenomenon is the different extent of the anisotropy in the two paints used. Going from $\alpha = 0$ to $\alpha = 70$ degrees, we have signal attenuations of 28% or paint type A and 7% for paint type B. The calibration factor k is usually determined in one part of the specimen with a zero or near zero angle of view. The calibration factor thus obtained is also used, however, on points of the tested object in which the angle of view is other than zero. Therefore the stress is always underestimated when there is an angle of view other than zero. With paint type B, however, this underestimation can be reduced to less than 10% for angles of up to 70°.

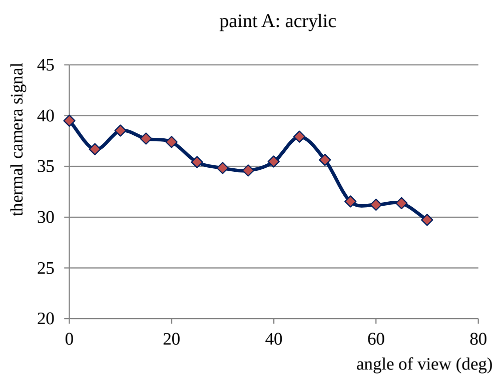

Fig. 3 Output of the differential camera with the varying of the angle of view for paint type A (acrylic)

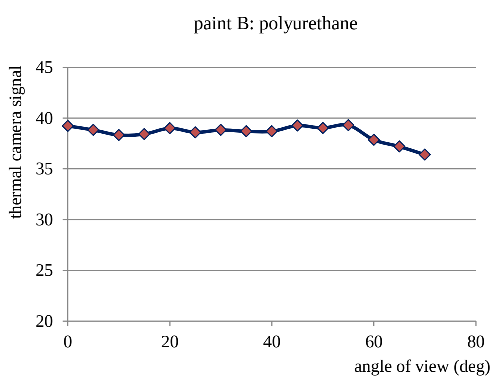

Fig. 4 Output of the differential camera with the varying of the angle of view for paint type B (polyurethane)

5.2 Tests for the analysis of the effects of the angle of view

These tests were conducted in order to evaluate the variation of the output of the differential thermographic camera with the varying of the load frequency in a painted specimen, both in one of its areas with uniform stress and in a second area with a stress gradient around a hole. The load frequency range examined goes from 1 to 15 Hz in 1 Hz steps. The steel specimen perforated at the center has two advantages: it allows the simultaneous detection of the effect of frequency with and without a stress gradient, and the maximum stress in the hole area can also be evaluated theoretically using known equations. The differential thermographic camera output was captured in a rectangular area far from the hole, in which there is a uniform stress. The mean spatial output signal in this area is called $S_{UNIFORM}$. The signal maximum near the hole was then determined. This operation is performed by measuring the profile of the differential thermographic camera output in a line centered on the hole (Fig. 6).

The values for $S_{UNIFORM}$ obtained at the various frequencies are shown in the diagram of Fig. 7.

For the painted specimens as well, there is clearly signal attenuation due to heat exchanges with the environment. In order to better illustrate this phenomenon, the differential thermogram images for the different frequencies are shown in Fig. 8. It can be seen that passing from a frequency of 15 Hz to 1 Hz there is a 16% attenuation of the $S_{UNIFORM}$ signal.

The trend of S_{MAX} at the different frequencies, determined as the average of at least three captures on the interrogation lines around the hole, is shown in Fig. 9. The reduction of the S_{MAX} signal is about 22%, passing from a frequency of 15 Hz to 1 Hz.

It is interesting to consider the relationship between the thermal camera signal for the uniform stress area and the signal for the point of maximum stress, which is also the maximum stress gradient point, that is, the ratio

$$R = \frac{S_{MAX}}{S_{UNIFORME}} \tag{8}$$

The trend of this ratio R with the varying of the frequency is shown in the graph in Fig. 10.

Two areas can be identified on this graph: one for frequencies greater than a threshold frequency ν_r equal to the specimen analyzed here at about 3 Hz, in which the ratio R oscillates slightly around the average value of 2.34, which corresponds to the theoretical value at less than 5%.

This suggests a consideration: despite the fact that when the frequency decreases, the specimen always transfers more heat to the environment, the signal attenuation in the various areas occurs uniformly. This is because the areas most stressed are also the warmest ones, thus they lose more heat than the less stressed areas, but always to such an extent that R remains constant. At frequencies lower than 3 Hz, the ratio R instead has a highly variable frequency trend.

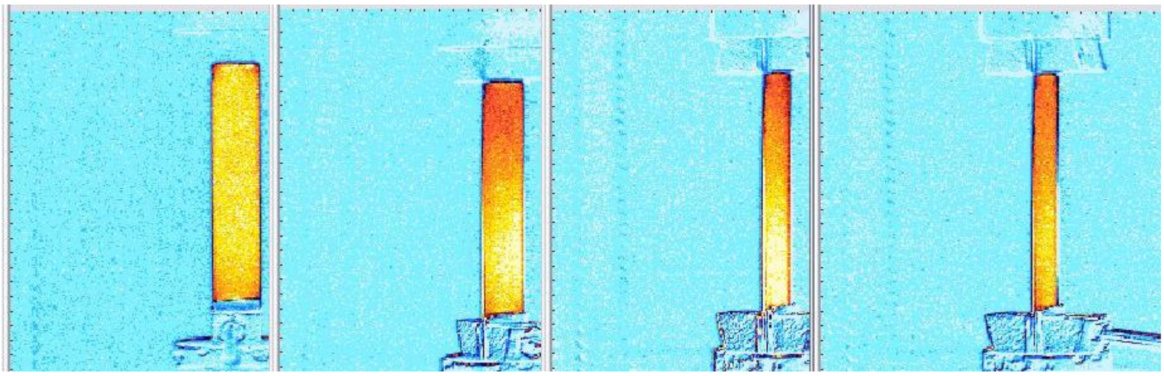

Fig. 5 Attenuation of the thermal signal with the increasing of the angle of vie

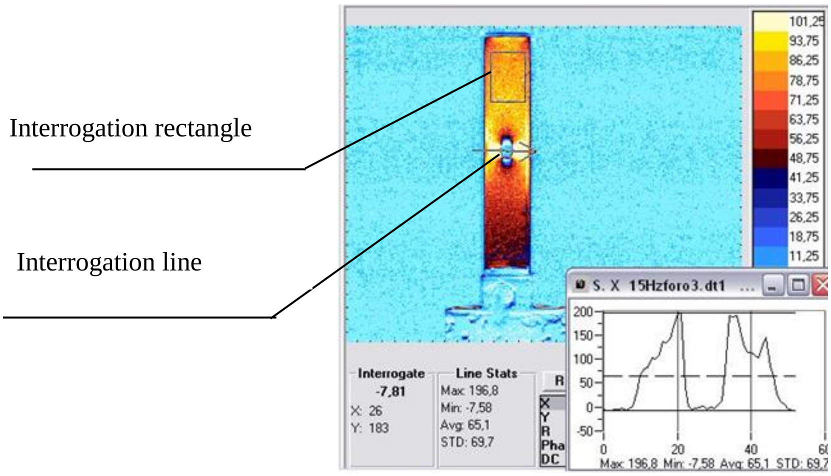

Fig. 6 Rectangle on which $S_{UNIFORM}$ is measured and interrogation line for determining S_{MAX} around the hole

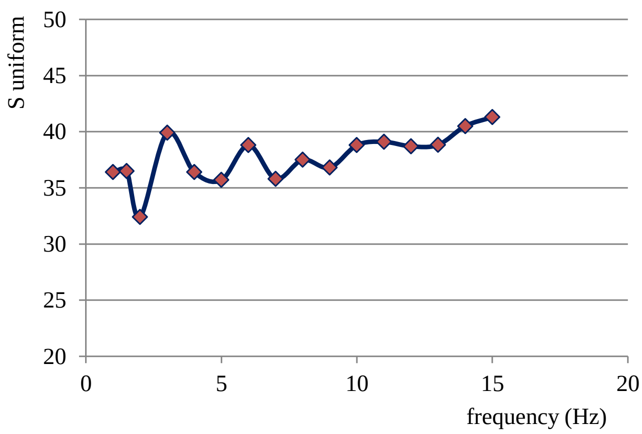

Fig. 7 Trend of the differential thermographic camera output signal for the area with uniform stress, with the varying of the frequency

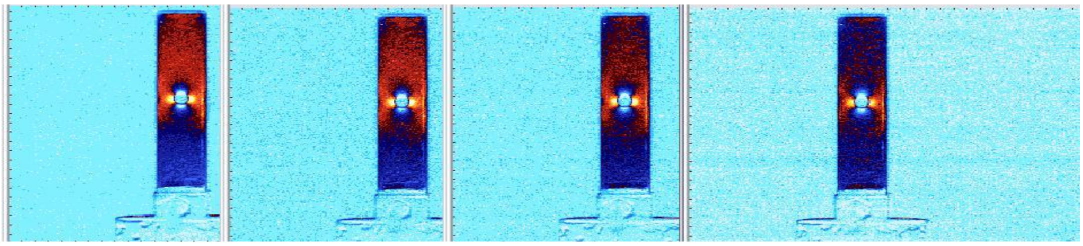

Fig. 8 Attenuation of the differential thermographic camera output with the varying of the angle of view

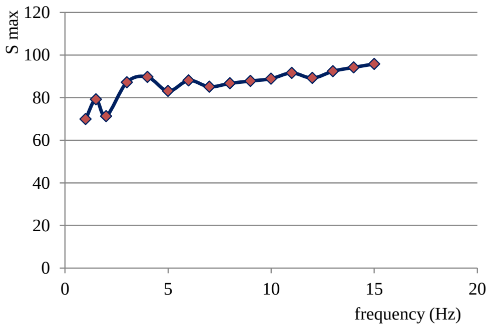

Fig. 9 Trend of the thermal camera output signal for the point of maximum stress, with the varying of the load frequency

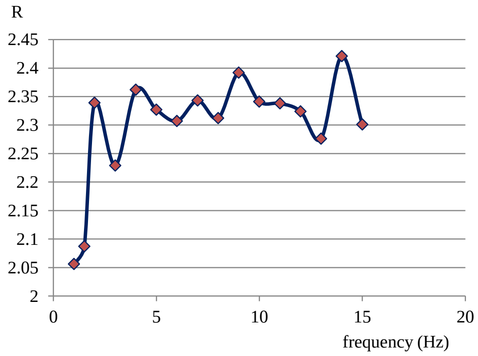

Fig. 10 Trend of the ratio R with the varying of the frequency

Therefore the attenuation of S_{MAX} and of $S_{UNIFORM}$ no longer occurs uniformly over the surface of the object being tested. This demonstrates that the phenomenon of heat conduction to the outside is superposed by the phenomenon of heat conduction between different points of the specimen, caused by the stress gradient. Indeed, this abrupt decrease of S_{MAX} is not attributable to the phenomena of heat transfer toward the outside, since otherwise it would have regarded $S_{UNIFORM}$ as well. In such test conditions, the calibration factor k thus varies from point to point, causing considerable degrees of uncertainty and the risk of underestimating stress concentrations and incision factors on the objects being tested. In the case of the perforated steel bar studied here, it was seen that when working with a load frequency greater than 1.5 Hz, an underestimate error of less than 10% is made. As regards the threshold frequency ν_r, it should be specified that there are many factors that influence its value, such as: type of material, thermal diffusion and, obviously, the stress gradient. Thus from an experimental perspective, it is best, when possible, to carry out several tests at increasing frequencies to evaluate whether or not the stress distribution changes in the areas with the highest gradient, i.e., to evaluate experimentally whether we are above the aforesaid limit.

6. Conclusions

This paper illustrated the thermoelastic technique for the contactless measurement of stress fields on structural elements stressed by dynamic loads. The main causes of uncertainty were theoretically and experimentally identified. The following conclusions can be drawn:

- the differential thermographic camera output signal varies with the varying of the angle of view and of the type of paint used. The tests showed that the output signal can be reduced even of 30% when the angle of view is about 70°;
- the attenuation of the output signal is also affected by the type of paint used for testing and is especially significant for large angles of view. Therefore it is important to choose a paint that has a low impact on the reduction of the output signal for the following reason. In fact the calibration factor k is usually determined in one part of the specimen with a zero or near zero angle of view. The use of calibration factor thus determined, on points of the tested object in which the angle of view is other than zero, gives stresses underestimated;
- the output signal is also variable with the load frequency. The test showed a reduction of the signal in areas with uniform stresses and in those prone to stress concentrations. It was shown that the measurement technique may underestimate the highest levels of stress, especially where there are significant gradients or highly thermally conductive materials.

Based on the tests and analyses performed, it was possible to define optimal measurement methods for reducing the effects of the main disturbance inputs at levels that can be considered acceptable for the various applications. Using steel specimens, some limits were quantitatively defined for measurement and testing parameters that are able to reduce these underestimation risks to less than 10% for the most common usage conditions, for example by optimizing the angle of view, using appropriate layers of paint, suitably choosing the load frequency of the object being tested, and the frequencies at which the calibrations are to be made.

References

Arefi, M. and Zenkour, A.M. (2017), "Nonlinear and linear thermo-elastic analyses of a functionally graded spherical shell using the Lagrange strain tensor", *Smart Struct. Syst*., **19**(1), 33-38.

Barone, S. and Patterson, E.A. (1998), "An iterative, finite difference method for post-processing thermoelastic data using compatibility", *J. Strain Anal. Eng. Des.*, **33**(6), 437-447.

Brouckaert, J.F., Marsili, R. and Rossi, G. (2012), "Development and experimental characterization of a new non contact sensor for blade tip timing", *Proceedings of the 10th International Conference on Vibration Measurements by Laser and Noncontact Techniques - AIVELA*, Ancona, Italy, June. Conference Proceedings Volume 1457, 61-68 DOI: 10.1063/1.4730543.

Brustenga, G., Marsili, R., Moretti, M., Pirisinu, J. and Rossi, G. (2005), "Measurement on rotating mechanical component by thermoelasticity", *J. Appl. Mech. Mater*., August. ISBN 0-87849-987-3 ISSN 1660-9336. SCOPUS: 2-s2.0-33745170726

Cardelli, E., Faba, A., Marsili, R., Rossi, G. and Tomassini, R. (2015), "Magnetic nondestructive testing of rotor blade tips", *J, Appl, Phys,*, **117**, 17A705. doi: 10.1063/1.4907180.

D'Aponte, F., D'Emilia, G., Lupinetti, S., Natale, E. and Pasqualoni, P. (2015), "Uncertainty of slip measurements in a cutting system of converting machinery for diapers production", *Int. J. Metrol. Qual. Eng.*, **63**(304), 1-6.

D'Emilia, G., Di Rosso, G., Gaspari, A. and Massimo, A. (2015), "Metrological interpretation of a six sigma action for improving on line optical measurement of turbocharger dimensions in the automotive industry", *Proceedings of the Institution of Mechanical Engineering: Part D*, J. *Automobile Eng.*, **229**(2), 261-269, DOI: 10.1177/0954407014539671.

D'Emilia, G., Razzè, L. and Zappa, E. (2013), "Uncertainty evaluation of high frequency image-based vibration measurement", *Measurement*, **46**(8), 2630-2637.

D'Emilia, G., Lucci, S., Natale, E. and Pizzicannella, F. (2011), "Validation of a method for composition measurement of a non-standard liquid fuel for emission factor evaluation", *Measurement*, **44**, 18-23.

Ezzat, M.A. and El-Bary, A.A. (2016), "Modeling of fractional magneto-thermoelasticity for a perfect conducting materials", *Smart Struct Syst*., 18(4), 707-731.

Garg, M., Sharma, S., Sharma, S., Mehta, R. (2016), "Non-contact damage monitoring technique for FRP laminates using guided waves", *Smart Struct Syst*., **17**(5), 795-817.

Garinei, A. and Marsili, R. (2014), "Development of a new capacitive matrix for a steering wheel's pressure distribution measurement", *Int. J. Ind. Ergonomics*, **44**(1), 114-119 doi: 10.1016/j.ergon.2013.11.012.

Garinei, A. and Marsili, R. (2014), "Thermoelastic stress analysis of the contact between a flat plate and a cylinder", *Measurement: J. Int. Measurement Confederation*, **52**(1), 102-110. http://dx.doi.org/10.1016/j.measurement.2014.03.005.

Garinei, A. and Marsili, R. (2013), "Design of an optical measurement system for dynamic testing of electrospindles", *Measurement*, **46**(5), 1715-1721. DOI information: 10.1016/j.measurement.2013.01.006, ISSN: 0263-2241, Elsevier Science.

Garinei, A. and Marsili, R. (2012), "A new diagnostic technique for ball screw actuators", *Measurement*, **45**(5), 819-828, ISSN: 0263-2241 DOI: 10.1016/j.measurement.2012.02.23.

Grigg, J.S., Dulieu-Barton, J.M. and Shenoi, R.A. (2000), "Validation of a complex composite construction using thermoelastic stress analysis", *Proceedings of the SEM IX International Congress on Experimental Mechanics*, Orlando, Florida, June.

Harish G., Szolwinski M.P., Farris T.N. and Sakagami T. (2000), "Evaluation of fretting stress through full-field temperature measurement", ASTM STP 2000.

Harwood, N. and Cummings, W.M. (1991), "Thermoelastic Stress Analysis", Adam Hilger.

Ju, S.H., Lesniak, J.R. and Sandor, B.I. (1997), "Numerical simulation of stress intensity factors via the thermoelastic technique", *Exper. Mech.*, **37**(3), 278-284.

Kim, H., Kang, D. and Kim, D. (2017), "Mechanical strength of FBG sensor exposed to cyclic thermal load for structural health monitoring", *Smart Struct Syst*., **19**(3), 335-340.

Lesniak, J.R. (1993), "Thermoelastic data improvements", *Proceedings of the SEM Spring Conference on Experimental Mechanics*, Dearborn, Michigan.

Logozzo, S., Kilpela, A., Makynen, A. and Zanetti, E. (2014), "Recent advances in dental optics- part-II: Experimental tests for a new intraoral scanner", *Opt. Laser Eng.*, **54**, 187-196.

Loktionov, A.P. (2016), "A measuring system for determination of a cantilever beam support moment", *Smart Struct. Syst*., **19**(4), 431-439. DOI : 10.12989/sss.2017.19.4.431

Offermann, S., Beaudoin, J.L., Bissieux, C. and Frick, H. (1997), "Thermoelastic stress analysis under non-adiabatic conditions", *Exper. Mech.*, **37**(4), 409-413.

Reifsnider, K.L. and Williams, R.S. (1974), "Determination of fatigue-related heat emission in composite materials", *Exper. Mech.*, 479-485.

Rocca, R. and Bever, M.B. (1950), "The thermoelastic effect in Iron and Nickel (As a Function of Temperature)", *Trans. AIME*, **188**, 327-333.

Rossi, G., Flori, R., Marsili, R. and Becchetti, M. (2009), "Stress and strain measurements by image correlation and thermoelasticity", Society for Experimental Mechanics - SEM Annual Conference and Exposition on Experimental and Applied Mechanics, Volume 1, 2009, Albuquerque, NM, United States, June. ISBN: 978-161567189-2; 978-161567189-2 SCOPUS: 2-s2.0-73349141710.

Sakagami, T., Ogura, K. and Shoda, M. (1995), "Thermal sensing and imaging of the dry sliding contact surface", Orlando, Florida, SPIE.

Speranzini, E., Marsili, R., Moretti, M. and Rossi, G.L. (2017), "Image analysis technique for material behavior evaluation in civil structures", *Materials*, **10**, 770. doi:10.3390/ma10070770

Speranzini, E., Agnetti, S. and Corradi, M. (2016), "Experimental analysis of adhesion phenomena in fibre-reinforced glass structures", *Composites part B*, **101**, 155-166. DOI: 10.1016/j.compositesb.2016.06.074.

Speranzini, E. and Agnetti S. (2014), "The technique of digital image correlation (DIC) to identify defects in glass structures", *Struct Control Health Monit.*, **21**(6), 2015-2029, DOI: 10.1002/stc.1629.

Speranzini, E. and Agnetti, S. (2013), "Post-cracking behavior of reinforced glass beams", *Proceedings of the COST Action TU0905, Mid-term Conference on Structural Glass*. Poreč, Croatia, April.

Speranzini, E. and Agnetti, S. (2012), "Structural performance of natural fibers reinforced timber beams", *Proceedings of the 6th International Conference on FRP Composites in Civil Engineering—CICE2012*, Roma, Italy, June. Scopus: 2-s2.0-84924402118.

Speranzini, E. and Tralascia, S. (2010), "Engineered lumber: LVL and solid wood reinforced with natural fibres", *Proceedings of the WCTE-Word Conference on Timber* Engineering, Trento, Italy, June. Scopus: 2-s2.0-84870414692.

Szolwinski M.P., Harish G. and Farris T.N. (1999), "In-Situ measurement of near surface fretting contact temperatures in an aluminium alloy", *J. Tribology*, **121**.

UNI CEI ENV 13005 (2000), "Guide to the expression of uncertainty in measurement" July.

Wong, A.K., Dunn, S.A. and Sparrow, J.G. (1988), "Residual stress measurement by means of the thermoelastic effect", *Nature*, **332**(6165), 613-615.

Zanetti, E.M. and Audenino, A.L. (2010), "Differential thermography for experimental, full-field stress analysis of hip arthroplasty", *J. Mech. Medicine Biology*, **10**(3), 515-529.

Zhou, W., Li, H., Dong, Y. and Wang, A. (2016), "Sensing properties of optical fiber sensor to ultrasonic guided waves", *Smart Struct. Syst.*, **18**(3), 471-484.

FC